BAND RATIOS AS A RECONNAISSANCE TOOL FOR HYPERSPECTRAL DATA

Brian S. Penn
Boeing-Autometric
Colorado Springs, Colorado
brian.s.penn@boeing.com

INTRODUCTION

There are now established procedures for extracting information from hyperspectral imagery data. The Environment for Visualizing Images (ENVI) from Research Systems, Inc. it the *defacto* hyperspectral image processing software package. The following are general steps for exploiting hyperspectral imagery (HSI) data when using ENVI:

1. Compensate for atmospheric interference. The most commonly used program is the Atmospheric Removal (ATREM) program (Gao and Goetz, 1990; CSES, 1999; Gao, Heidbrecht, and Goetz, 1999).
2. Reduce the dimensionality of the data set using a Minimum Noise Transformation Boardman and Kruse (1994);
3. Find the purest pixels (apices for a hypervolume enclosing the *N*-dimensional dataset) in the hypercube representing end-members in the data set and selecting the pixels with the highest probability of being end-members (Boardman, Kruse, and Green, 1995);
4. Visualizing the highest probability end-member pixels by projecting them into two-dimensional space (Boardman, Kruse, and Green, 1995);
5. Linearly unmix the remaining pixels based on the end-members. Map the results to show relative proportions using Matched Filters, Mixture Tuned Matched Filtering™, Spectral Angle Mapper™, or some other classification procedure.

This is the most widely used approach for working with hyperspectral data by researchers external to the U.S.G.S. Spectroscopy Laboratory. The U.S.G.S. Spectroscopy Laboratory developed its own HSI image processing software. Their program, called Tetracorder, uses a significantly different paradigm to extract information from HSI data. Both ENVI and Tetracorder have much in common, but there are significant fundamental differences. Some of those differences are explored in Penn and Livo (2001).

There are other ways to extract information from HSI data. One such method uses ratios of hyperspectral data. Band ratios have been used extensively for manipulating multispectral data, but have never been embraced by the HSI community. The purpose of this paper is to present a quantitative basis for using band ratios, focusing on the optimal conditions for using band ratios.

Band ratios represent an opportunity to eliminate false-assumptions and over generalizations from the process of atmospheric removal and subsequent spectral processing. In fact, it is shown in this paper how the proper use of band ratios obviates the need for atmospheric correction for HSI data.

RADIOMETRIC CONCEPTS

The total solar irradiance reaching the earth's surface is equal to:

$$E_g = \int_{\lambda_1}^{\lambda_2} (E_{0\lambda} T_{\theta_0} \cos\theta_0 + E_{d\lambda}) d\lambda \quad (1)$$

where E_g is the global irradiance on the surface, $E_{0\lambda}$ is the spectral solar irradiance at the top of the atmosphere, $T\theta_0$ is the atmospheric transmittance at angle θ, $E_{d\lambda}$ is the spectral diffuse sky irradiance

Radiance is defined as the sum of the energy measured at the sensor including contributions from all the areas within the instantaneous field of view (IFOV), i.e., the target, surrounding areas, and the various scattering components of the atmosphere. The total radiance reaching the sensor (L_S) is the sum of the light from the target (L_T) and the contribution from the path radiance (L_P). Therefore,

$$L_S = L_P + L_T \quad (\text{W/m}^2\text{/sr}) \quad (2)$$

and,

$$L_T = L_I + L_A \quad (\text{W/m}^2\text{/sr}) \quad (3)$$

where L_I is equal to the radiance directly reflected from the target and L_A is the atmospheric contribution to the radiance coming from the target. Path radiance is the contribution to the total radiance at the sensor derived from scattering in the atmosphere and light from areas other than the target area. Also, the path radiance is not simply equal to the atmospheric contribution to the L_I, $L_A \neq L_P$, passing through the atmosphere to the sensor. A summarization of methods for computing path radiance are found in Turner and Spencer (1972), Turner (1975, 1978), and Foster (1984).

The actual amount of radiance reflected to the sensor from the target is very small and is equal to:

$$L_T = \tfrac{1}{\pi} \int_{\lambda_1}^{\lambda_2} R T_{\theta_V} \left(E_{0\lambda} T_{\theta_0} \cos\theta_0 + E_{d\lambda}\right) d\lambda \quad (\text{W/m}^2\text{/sr}) \quad (4)$$

Vincent (1997) modifies equation (4) by adding a unitless multiplicative *S* factor called the "shadow/slope" factor. The *S* factor is closely related to the bi-directional reflectance function (BDRF), i.e., all surfaces are non-Lambertian reflectors. Most equations concerning atmospheric compensation ignore this aspect of radiance calculations. The *S* factor is unique for each part of the earth's surface and makes a significant contribution to L_S. Vincent (1997) also adds sensor specific contributions to the L_S, including electronic gain as a multiplicative factor and electronic offset as an additive factor.

No known atmospheric models account for the contributions of these last three factors primarily because the first is completely unknown and the last two are sensor dependent. If the sensor is calibrated, then the gains and offsets for each channel are known and can be applied to the data. Vincent and Thomson (1972) helped pioneer the use of band ratios to deal with the *S* factor in HSI data.

DISCUSSION – CONVERTING RADIANCE TO REFLECTANCE

The previous sections on atmospheric compensation are designed to outline common thinking for converting radiance values to reflectance values. Many members of the HSI community work exclusively in the reflectance domain to the exclusion of radiance. Significant misunderstandings have occurred over the veracity of using radiance versus reflectance data. The basis for the current bias toward reflectance data has its roots in the origins of HSI. The "founders" of hyperspectral imaging at JPL (Gregg Vane, Alexander Goetz, Larry Rowan, etc.) and Johns Hopkins (Graham Hunt and John Salisbury) either were geologists by training, or had a strong geologic mindset. Consequently their interests in spectroscopy were directed to minerals. Using a Nicolet 5 DXB, Nicolet System 510 interferometer spectrometer or a Beckman 5270 Spectrometer (2 nm spectral sampling resolution) reflected light spectrum for specific minerals were measured under laboratory conditions. Once the airborne imaging spectrometers were built and flown, the desire was to relate the signals collected at altitude to the laboratory spectra for individual minerals. The logical approach was to model and remove the atmospheric contribution from the radiance data to make the signal look more like the spectra collected in the laboratory. Atmospheric models such as 6S, LOWTRAN, MODTRAN, etc. were developed to remove the atmospheric effects based on radiative transfer theory. Most atmospheric models such as LOWTRAN, MODTRAN, etc., generate a series of offsets and gains to be applied across an entire image to convert radiance data to reflectance data.

The heterogenous nature of the Earth's atmosphere requires atmospheric corrections be done on a pixel-by-pixel basis (Gao and Goetz, 1990). The development of the Atmosphere Removal (ATREM) program resulted from this idea (Gao, Heidebrecht, and Goetz, 1999). ATREM is presented here as an example of one of the premier atmospheric compensation models. Other models are based on similar physical principles and/or have less fidelity than ATREM.

ATREM has three specific assumptions (Gao, Heidebrecht, and Goetz, 1999): 1) the reflecting surface is horizontal; 2) the surface is a Lambertian reflector, i.e., light is reflected equally in all directions; and 3) CO_2, CO, CH_4, O_2, O_3, and N_2O are uniform across a hyperspectral scene (H_2O varies both spatially, vertically, and temporally).

ATREM has two shortcomings:

1. ATREM overcorrects in the blue wavelengths. The over correction in the blue wavelengths must be manually fixed.
2. To correctly generate reflectance data using ATREM, a user must go to the field and collect representative spectra using a handheld spectroradiometer either during the overflight or as soon as possible thereafter. Using the spectra gathered in the field, a series of gains and offsets are generated and applied to the output reflectance data from ATREM.

As stated in the ATREM User's Manual, ATREM uses an "approximate atmospheric radiative transfer model." Of the thirty or so atmospheric gases, only seven (H_2O, CO_2, CO, CH_4, O_2, O_3, and N_2O) have significant features in the 0.4-2.5 um region. ATREM focuses on removing the effects of H_2O because, with few exceptions, water dominates atmospheric absorptions for wavelengths from 0.4-2.5 μm. Also, the strength of the H_2O absorption features are such that they hide weaker absorption features from other gases (Clark, 1999). ATREM calculates the water content for each pixel by using a three-channel ratioing technique for water vapor features centered at 0.94 μm and 1.14 μm. Scattering terms for surface reflectance are calculated using the 6S code of Vermote, et. al. (1996) and a user selected aerosol model. Atmospheric transmittance for each gas is calculated using the Malkmus (1967) narrow band model and a user-selected standard atmospheric model (temperature, pressure, and vertical water vapor distribution).

ATREM relies on a number of assumptions that are only correct to a first approximation and, as hyperspectral instruments achieve greater spatial resolution, these assumptions will produce more pronounced output errors. Software programs like ENVI contain methods such as the Empirical Flat Field Optimal Reflectance Transformation (EFFORT) to remove cumulative corrections associated with calibration and atmospheric correction associated with ATREM (Boardman, 1998). Another source of error in ATREM is selection aerosol and standard atmosphere models to derive a reflectance spectrum by the user. If the user is not very adept with ATREM, then the resultant spectrum may not correlate with actual surface reflectance. In addition, small absorption features may be completely obliterated based on an incorrect assumption or poorly selected model. ATREM is still one of the best methods for compensating for atmospheric contributions to hyperspectral imagery, but it does have limitations, as do all radiative tranfer-based models. The solution to these shortcomings may be found in the empirically simple method of ratioing bands.

BAND RATIOS

Under certain conditions, ratioing two bands can eliminate the shortcomings of radiative transfer models and greatly expedite the processing and exploitation of hyperspectral data. Band ratios have been used extensively since the early 1970s (Vincent and Thomson, 1971; Vincent and Thomson, 1972; Vincent, 1973, Rowan et. al., 1974; Goetz, 1975; Ashley and Abrams, 1980; Rowan and Kahle, 1982; Podwysocki et. al., 1983; Fraser and Green, 1987; Crippen, 1988; Davis et. al., 1989; Rowan et. al., 1992; Crippen, 2001) to extract information from satellite imagery and airborne spectral scanners. These applications have been mostly constrained to multispectral imagery data, although recent work (Vincent, 1997; Clark, 1999; Mustard and Sunshine, 1999; Jengo, 2001) suggests that band ratios are equally applicable to HSI data.

Band ratios cannot be done haphazardly. Crippen (1988 and personal communication) detailed the problems that can occur with band ratioing and how to easily fix them. Vincent (1997, and personal communication) outlines a similar approach that essentially involves performing a dark subtraction on each band prior to ratioing the bands. Performing a dark subtraction removes additive radiance terms (electronic noise and

offset, and atmospheric path radiance) (Jengo, 2001). Using a dark subtraction assumes that the lowest Digital Number (DN) for each band should be equal to zero and the reason the first DN ≠ 0 is due to atmospheric contribution, i.e., scatter, local slope/shadow, *S*, factor, and electronic gains and offsets. This is especially true for the near infrared wavelengths. Clear water absorbs 100% of the near infrared light, but often a spectrometer shows a DN value for water greater than zero. The atmospheric contribution for that particular channel, due to atmospheric scattering, is its DN, because there should be no reflectance value for that wavelength over water.

Another important rule for band ratios is that the bands being ratioed must not differ in wavelength by more than a few tens of nanometers. If the bands being ratioed are significantly far apart, then the atmospheric contribution, and sensor gains and offsets could be very different, invalidating the results of the ratio. For this reason most band ratios applied to HSI data are located such that one band lies in the center of a known sharp absorption feature and the other band lies nearby on the shoulder of the feature.

Stated another way, L_S values can be calculated in the following manner:

$$L_S = \int_{\lambda_1}^{\lambda_2} (L_P L_I T\theta_V) d\lambda \qquad (5)$$

where L_{S_1} and L_{S_2} are sampled close together, $L_{P_1} \approx L_{P_2}$ and $T\theta_{V_1} \approx T\theta_{V_2}$, reducing the ratioed values to $\frac{L_{I_1}}{L_{I_2}}$. From this reasoning, it is understandable why band ratios eliminate the need for atmospheric corrections as long as the user knows where specific and characteristic absorption features are found in a spectrum.

Interestingly, there is no doubt as to the efficacy of using band ratios on multispectral data. There is no controversy despite the fact that the atmosphere responds to photons non-linearly over the 0.7-1.0 μm wide bands commonly ratioed in multispectral imagery data. When band ratios are utilized in HSI data, based on the rules given above, they are spectrally so close together that atmospheric effects should certainly be nearly equal for the two bands. Assumptions such as a horizontal surface and a Lambertian reflector are empirically addressed by band ratios because each is effectively the same for two closely-spaced bands (see equation 5). Band ratios are not limited to radiance data alone; they work equally well on reflectance data assuming that atmospheric compensation was done correctly.

Band ratios are a coarse, quick-check tool for examining radiance data (figure 1). This technique enables analysts to verify the presence of known materials based on absorption features. However, band ratios are not the answer to questions such as which cation, Mg^{2+} or Na^{+}, is substituted into the lattice of montmorillonite. This type of detailed chemical analysis requires reflectance data.

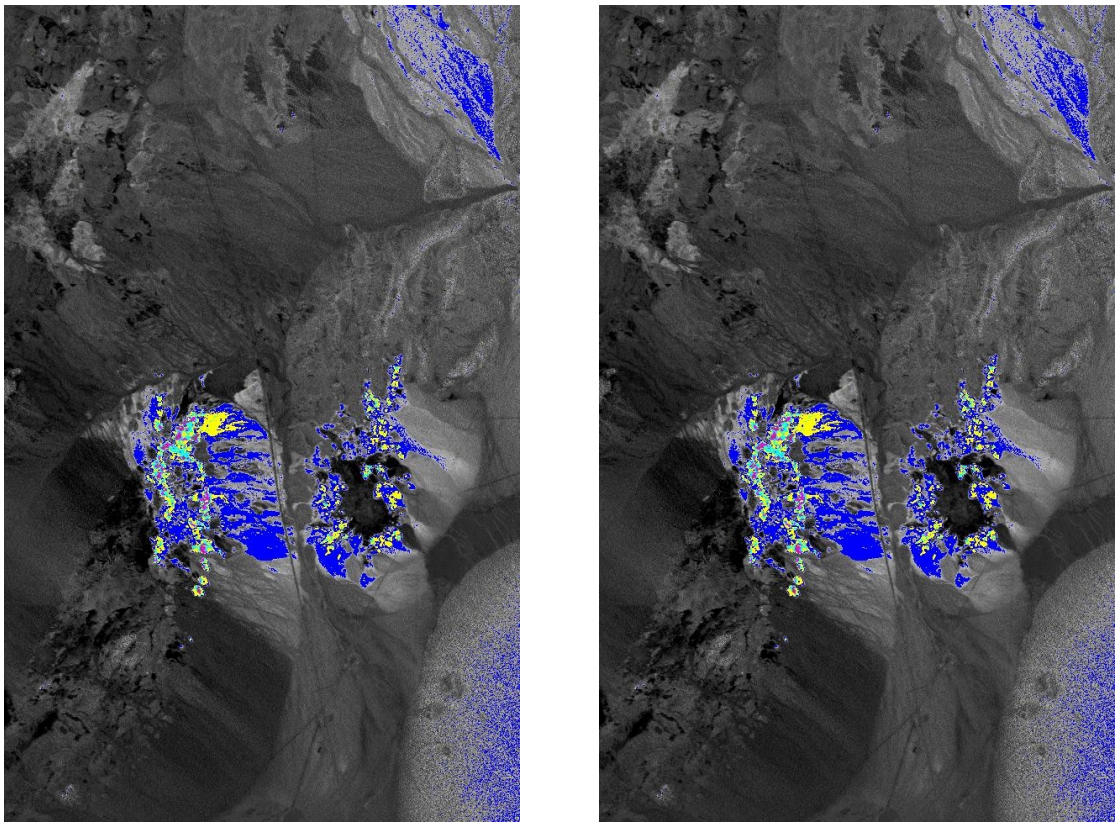

1a 1b

Figure 1 – Results of band ratios to find alunite in Cuprite 1995 AVIRIS scene.
a) radiance data, b) U.S.G.S. radiative transfer ground calibrated reflectance data

DERIVATIVE RATIO ALGORITHM

Further supporting the validity of band ratios is the work of Philpot's (1991) using derivative ratios. Derivatives have been used to analyze multispectral and hyperspectral data to extract information about minerals, plants, and soils (Foster, 1984; Bruce and Li, 2001). This more complex implementation of the band ratio concept is based on taking derivatives of the radiative transfer equation called the Derivative Ratio Algorithm (DRA) (Philpot, 1991). The goal of this approach is to determine the conditions for which the derivative algorithm is not subject to atmospheric interference. DRA uses the ratio of the *n*th derivative at λ_1 over a second derivative at λ_2. DAR demonstrated under certain conditions to obviate the need for atmospheric compensation. Equation (2) is modified by Philpot (1991) to the following:

$$L_s = TE_d R_t + L^* \tag{6}$$

Where T is atmospheric transmittance, E_d is the downwelling irradiance, R_t is target reflectance, and L^* is atmospheric path radiance. The first derivative of equation (6) is

$$\frac{dL_s}{d\lambda} = TE_d R_t \left[\frac{dRt}{R_t d\lambda} + \frac{dE_d}{E_d d\lambda} + \frac{dT}{Td\lambda} \right] + \frac{dL^*}{d\lambda}. \quad (7)$$

When the slope of the curve is sufficiently steep, the reflectance term dominates the equation yielding

$$\frac{dL_s}{d\lambda} \approx TE_d \frac{dR_t}{d\lambda}. \quad (8)$$

Eliminating the effects of the atmospheric contribution in equation (8) occurs only under certain conditions and wavelengths such that

$$\frac{T(\lambda_1)E_d(\lambda_1)}{T(\lambda_2)E_d(\lambda_2)} = 1. \quad (9)$$

If equation (9) holds, then the ratio of the first derivatives is equal to the ratio of the reflectance values at wavelengths λ_n, i.e.,

$$\frac{(dL_s/d\lambda)|\lambda_1}{(dL_s/d\lambda)|\lambda_2} \approx \frac{(dR_t/d\lambda)|\lambda_1}{(dR_t/d\lambda)|\lambda_2}. \quad (10)$$

Equation (8) can be generalized for all derivatives

$$\frac{d^n L_s}{d\lambda^n} \approx TE_d \frac{d^n R_t}{d\lambda^n}. \quad (11)$$

Equation (11) is further generalized by Bruce and Li (2001) to:

$$\frac{df}{d\lambda} = \frac{f(\lambda_2) - f(\lambda_1)}{\lambda_2 - \lambda_1} = \frac{f(\lambda_2) - f(\lambda_1)}{\Delta\lambda} \quad (12)$$

The $\Delta\lambda$ is critical because of inherent atmospheric heterogeneities. The maximum acceptable value for $\Delta\lambda \leq 50$ nm (Philpot, 1991). The other critical factor is that the curve must be sufficiently steep for this method to be valid. This is also true for band ratios in general; they function best for sharp absorption features. The DRA is more complex, yet consistent with simple band ratios.

CONCLUSIONS

Applying band ratios to radiance data has significant advantages over converting radiance data to reflectance but there remain some limitations:

1) A dark subtract must be performed on the imagery data. The requisite for a dark subtract is a large dataset with at least some areas with low reflectance values;

2) The DRA suggests that bands used for ratioing must be ≤ 50 nm apart to ensure that the numerator and denominator multiplicative factors are ≈ 1;
3) Requires sharp features associated with SWIR portion of the electromagnetic spectrum;
4) Susceptible to calibration errors.

Once these conditions are met, band ratioing provides a tool for quick assessment of materials present in hyperspectral data.

Performing high-quality utilization of hyperspectral data requires considerable effort to remove atmospheric interference effects. This type of fidelity requires accessing the target area as near as possible to the time of the sensor overflight to collect spectra using a hand-held spectrometer. Most computer programs to compensate for atmospheric interference are based on radiative transfer models of the atmosphere containing assumptions and generalizations regarding the atmosphere. Limiting the applicability of such models are there inability to account for non-Lambertian surfaces and sensor gains and offsets. Simple band ratios, when done properly, can efficiently produce high quality results from hyperspectral data.

REFERENCES

Ashley, R. P. and Abrams, M.J. 1980. Alteration mapping using multispectral images, Cuprite Mining District, Esmeralda County, Nevada, U.S.G.S. Open File Report 80-367, U.S. Geological Survey, Washington, D.C.

Boardman, J.W., and Kruse, F.A. 1994. Automated spectral analysis: A geologic example using AVIRIS data, north Grapevine Mountains, Nevada, in Proceedings of the 10th Thematic Conference on Geologic Remote Sensing, Environmental Research Institute of Michigan, Ann Arbor, Michigan, I – 407 – I – 418.

Boardman, J.W., Kruse, F.A., and Green, R.O., 1995. Mapping Target Signatures va partial unmixing of AVIRIS data in Summaries, 5th JPL Airborne Earth Science Workshop, JPL Publication 95-1, vol. 1, 23-26.

Boardman, J.W., 1998. Post-ATREM polishing of AVIRIS apparent reflectance data using EFFORT: a lesson in accuracy versus precision, in Summaries of the Seventh JPL Airborne Earth Science Workshop, Vol. 1, p. 53.

Bruce, L.M., and Li, J. 2001. Wavelets for Computationally Efficient Hyperspectral Derivative Analysis, IEEE Transactions in Geoscience and Remote Sensing, 39(7), 1540- 1546.

Clark, R. N. 1999. Spectroscopy of Rocks and Minerals, and Principles of Spectroscopy in Remote Sensing for the Earth Sciences: Manual of Remote Sensing, 3rd edition, volume 3, Rencz, A. N. (ed.), John Wiley and Sons, Inc., New York, New York, 707 pages.

Center for the Study of Earth from Space (CSES) 1999. Atmosphere Removal Program (ATREM) User's Guide, Version 3.1. 31p.

Crippen, R. E. 1988. The dangers of underestimating the importance of data adjustments in band ratioing, International Journal of Remote Sensing, 9(4):767-776.

Crippen, R.E. 2001. Unveiling the Lithology of Vegetated Terrains in Remotely Sensed Imagery, Photogrammetric Engineering & Remote Sensing, 67(8), 935- 943.

Davis, P.A., Mullins, K.F., Berlin, G.L., Al-Farasani, A.M., and Dini, S.M. 1989. Phosphorite exploration in the Thaniyat and Sanam districts, Kingdom of Saudi Arabia, using Landsat thematic mapper data. Proceedings of the 7th Thematic Conference on Remote Sensing for Exploration Geology, Vol. II, Environmental Research Institute of Michigan, Ann Arbor, Michgan, 1205-1221.

Foster, B. C. 1984. Derivations of Atmospheric Correction Procedures for Landsat MSS with Particular Reference to Urban Data, International Journal of Remote Sensing, vol. 5, 799-817.

Fraser, S.J, and Green, A.A. 1987, A software defoliant for geological analysis of band ratios. International Journal of Remote Sensing, 8, 525-532.

Gao, B. -C., and Goetz, A.F.H. 1990. Column Atmospheric Water Vapor and Vegetation Liquid Water Retrievals from Airborne Spectometer Data, Journal of Geophysical Research, 95, 3549-3564.

Gao, B.-C., Heidbrecht, K.G., and Goetz, A.F.H. 1999. Atmospheric Removal Program (ATREM) Users Guide Version 3.1: Center for the Study of Earth from Space (CSES), University of Colorado at Boulder, 31 p.

Goetz, A.F.H., 1975, Imaging for geothermal exploration, Geothermal Workshop on Geophysical Methods Applied to Detection, Delineation and Evaluation of Geothermal Resources, 13-18, Dept. of Geology and Geophysics,University of Utah, Salt Lake City, U. S. Geological Survey, Snowbird, Utah.

Jengo, C. 2001. Hyperspectral Imaging of Ancient Hydrocarbon Seeps, Wind River Basin, Wymoing. M.S. Thesis, Bowling Green State University, Bowling Green, Ohio, 202 p.

Malkmus, W. 1967. Random Lorentz Band Model with exponential-tailed S line intensity distribution function, Journal of the Optical Society of America, vol. 57, 323-329.

Mustard, J.F., and Sunshine, J. M. 1999. Spectral Analysis for Earth Science: Investigations Using Remote Sensing Data. In Remote Sensing for the Earth Sciences:

Manual of Remote Sensing, 3rd ed., Vol. 3., A. M. Rencz (ed.), John Wiley & Sons, New York, New York, 251- 306.

Penn, B.S., and Livo, K.E. 2001. Using AVIRIS Data to Map Geologic Signatures of Copper Flat Porphyry Copper Deposit, Hillsboro, New Mexico, in Proceedings of the Tenth JPL workshop on Airborne Earth Science Workshhop, Jet Propulsion Laboratory, California Institute of Technology, February 28 - March 2, 2001.

Philpot, W. D. 1991. The Derivative Ratio Algorithm: Avoiding Atmospheric Effects in Remotes Sensing, IEEE Transactions on Geoscience and Remote Sensing, 29(3), 350-357.

Podwysocki, M.H., Segal, D. B., and Abrams, M.J. 1983. Use of multispectral scanner images for assessment of hydrothermal alteration in the Marysvale, Utah mining areas, Economic Geology, 78, 675-687.

Rowan, L.C., Wetlaufer, P.H., Goetz, A.F.H., Billingsley, F.C., and Stewart, J.H. 1974. Discrimination of Rock Types and Detection of Hydrothermally Altered Areas in South-Central Nevada by Use of Computer-Enhanced ERTS Images, U.S.G.S. Professional Paper 883, U.S. Geological Survey, Washington, D.C., 35 p.

Rowan, L.C., and Kahle, A.B. 1982. Evaluation of .46-2.36 um multispectral scanner image of the East Tintic mining district, Utah for mapping hydrothermally altered rocks, Economic Geology, 77, 441-452.

Rowan, L.C., Pawlewicz, M.J., and Jones, O.D. 1992. Mapping Thermal Maturity in the Chainman Shale, near Eureka, Nevada, with Landsat Thematic Mapper images. American Association of Petroleum Geologists Bulletin, 76(7):1008-1023.

Turner, R. E. 1975. Signature Variations Due to Atmospheric Effects in Proceedings, 10th International Symposium on Remote Sensing of the Environment, Ann Arbor, MI, Environmental Research Institute of Michigan, 671-682.

_____ 1978. Elimination of Atmospheric Effects from Remote Sensing Data, in Proceedings, 12th International Symposium on Remote Sensing of the Environment, Ann Arbor, MI, Environmental Research Institute of Michigan, 783.

Turner, R.E. and Spencer, M.M. 1972. Atmospheric Model for Correction of Spacecraft Data in in Proceedings, 8th International Symposium on Remote Sensing of the Environment, Ann Arbor, MI, Environmental Research Institute of Michigan, 895-934.

Vermote, E., Tanre, D., Deuze, J.L., Herman, M., and Morcrette, J.J. 1996. Second Simulation of the Satellite Signal in the Solar Spectrum (6S), 6S User's Guide Version 1, NASA-GSFC, Greenbelt, Maryland, 134 pages.

Vincent, R. K, and Thomson, F. 1971. Discrimination of Basic Silicate Rocks by

Recognition Maps Processed from Aerial Infrared Data. In Proceedings of the Seventh International Symposium on Remote Sensing of the Environment, Ann Arbor, Environmental Research Institute of Michigan, 247-252.

Vincent, R. K., and Thomson, F. 1972. Rock Type Discrimination from Ratioed Infrared Scanner Images of Pisgah Crater, California. Science 175:986-988.

Vincent, R. K. 1973. A Thermal Infrared Ratio Imaging Method for Mapping Compositional Variation Among Silicate Rock Types. Ph.D. University of Michigan, Michigan.

_____ 1997. Fundamental of geological and environmental remote sensing. Prentice-Hall, Upper Saddle River, New Jersey, 366p.